Accepted in ApJ, November 2006.
Preprint typeset using LaTeX style emulateapj v. 10/09/06

MOLECULAR LINE SURVEY OF CRL 618 FROM 80 TO 276 GHZ AND COMPLETE MODEL

Juan R. Pardo, José Cernicharo & Javier R. Goicoechea
IEM - Departamento de Astrofísica Molecular e Infrarroja, CSIC, Serrano 121, E-28006 Madrid, Spain.

and

Michel Guélin
Institute de Radioastronomie Millimétrique, 30 rue de la Piscine, F-38406 Saint Martin d'Hères, France

and

Andrés Asensio
Instituto de Astrofísica de Canarias, E-38205, La Laguna, Tenerife, Spain
Accepted in ApJ, November 2006.

ABSTRACT

We present the complete data set, model and line identification of a survey of the emission from the C-rich protoplanetary nebula CRL 618 performed with the IRAM-30m telescope in the following frequency ranges: 80.25-115.75 GHz, 131.25-179.25 GHz, and 204.25-275.250 GHz. A selection of lines from different species has been used in previous works to derive the structure of the source, its physical conditions and the chemical abundances in the different gas regions. In this work, we have used this information to run a global simulation of the spectrum in order to check the consistency of the model and to ease the task of line identification. The total number of lines that have a correspondence in both data and model is ∼3100, although quite often in this object many lines blend into complex features so that the model, that takes into account line blending, is a key tool at this stage of the analysis. Of all the lines that we have been able to label, ∼55% of them belong to the different forms of HC_3N, and ∼18% to those of HC_5N. The density of remaining unidentified features above the 3σ limit is only one per ∼2.1 GHz (74 features), which is unprecedented in the analysis of this type of large millimeter-wave line surveys.

Subject headings: line identification - surveys - stars: post-AGB-stars: carbon-rich - stars: circumstellar matter - stars: individual: CRL 618 - ISM: molecules - radio lines: stars

1. INTRODUCTION

In order to study the evolutionary stages from Asymptotic Giant Branch (AGB) to Planetary Nebulae (PN), multiwavelength and multi-object data are necessary to reveal the key changes in physical conditions and chemical composition as completely as possible. Even so, the task is not trivial due to the many distinct environments that can be present in these C-rich or O-rich objects including: very fast winds and presence of shocks (Cernicharo et al. 1989; Davis et al. 2005; Bujarrabal et al., 2002), binarity (Sánchez-Contreras et al. 2004, De Marco et al. 2004), magnetic fields (Frank & Blackman 2004; Huggins & Manley 2005), late thermal pulses (Asplund et al. 1999, Pavlenko et al. 2004), etc... Molecular spectroscopy at millimeter, submillimeter and FIR wavelengths is a useful tool to study the early stages of this evolution because large carbon chain and metal containing molecules form in the atmospheres of late-type stars. This rich formation chemistry exists in C-rich objects due to the relatively high densities and the presence of dust and shocks created by significant mass loss (Cernicharo 2004). In addition, the potentially photodissociating radiation from the central star, when it changes its spectral type, is blocked in a compact inner region. As the evolution goes on, the shielding of high energy photons from the central star, that has evolved toward types A, B and O is less effective so that the molecular content in the envelope decreases greatly.

Electronic address: cerni,pardo@damir.iem.csic.es

The ideal targets to study the formation chemistry of large carbon-chain molecules are late type stars with significant mass loss (e.g., IRC+10216), protoplanetary nebulae (e.g., CRL 2688 and CRL 618) and very young planetary nebulae (e.g., NGC 7027). Herpin et al. (2001), performed a study using several CO lines across the mm and submm ranges in the latter four objects, taken as prototypes for the different steps of the AGB to PN evolution, aimed at determining the physical conditions prevailing for the molecular gas. Sánchez-Contreras et al. (2002, 2004) have undertaken a multiwavelength study of CRL 618. Cernicharo et al. (1996, 2001a,b) have explored the ISO data of CRL 618 and IRC+10216 with interesting findings such as the first evidence for the first aromatic molecule seen outside the solar system (C_6H_6 in CRL 618). Remijan et al. (2005) have performed a search for large molecules toward CRL 618 although no detection of biologically important molecules could be reported. Finally, Cernicharo et al. (2000) published a λ=2 mm survey of IRC+10216. Therefore, our motivation for the complete *Institute de Radioastronomie Millimétrique* (IRAM) 30 meter telescope survey of CRL 618, fully presented here, has been to gather the most complete molecular information on one particular stage (protoplanetary nebula, PPNe) of low-mass stellar evolution, of which CRL 618 is the best C-rich example. The data on their own have allowed a quite precise determination of physical conditions and molecular abundances in this object (Pardo et al. 2004, 2005; Pardo & Cernicharo 2006; hereafter P04, P05 and PC06). These pre-

vious works have allowed us to build a complete model to be compared with the whole data set, thus simplifying the task of isolating U-lines during the line identification process.

2. OBSERVATIONS SUMMARY

The CRL 618 IRAM-30m line survey was completed in 1994-2002. In order to keep the calibration of the spectra as consistent as possible, the observing procedure was kept unchanged through the years. Nevertheless, technical works at the telescope and varying atmospheric conditions are responsible for a relative calibration uncertainty of the order of 10%. This uncertainty in the calibration was based on observing the same lines at different epochs. The analysis of more than 15 lines in different vibrational states of HC_3N has allowed to notice a few scans with obvious calibration problems (less than 10 over more than 350 spectra, or <3%) most probably due to an erroneous calibration scan. Those few spectra were re-scaled based on the overall results of the rotational HC_3N ladders.

In order to avoid signal and image sideband confusion, image sideband rejection larger than 12 dB was used. Features that could be attributed to sideband contamination are only a few, generally related to a very intense line (CO, HCN, HNC, HCO^+,...) in the image side band. The pointing and focus were always checked on the target source and the peak level of the gaussians after the last correction of each pointing session has been used to study the spectral behavior of the millimeterwave continuum in CRL 618. The pointing itself was kept within 2" accuracy. The observations were carried out using the wobbler-switching mode with offsets of 60" and frequencies of 1 Hz, in order to obtain very flat baselines. The backends were two 512×1 MHz filter banks connected to the receivers operating below 200 GHz, and an autocorrelator with channel widths of 1.25 MHz connected to the receivers operating in the 1.3 mm window. System temperatures were typically 100-400 K at 3 mm, 200-600 K at 2 mm, and 300-800 K at 1.3 mm.

Complementary observations above 280 GHz have been carried out with the 10.4 m dish of the Caltech Submillimeter Observatory (Mauna Kea, Hawaii) and some of them have been used in the analysis presented in P04, P05 and PC06. The complete results above 280 GHz will be published elsewhere.

3. RESULTS

In order to illustrate the overall results of the survey we include here two tables (4 and 5) describing the molecules detected and the J_{up} or energy range in which the lines of a particular species are seen. Other species included in the model, although marginally or not detected, appear also in the same table. We also provide four figures showing the overall data and model in four spectral ranges, corresponding to those of the available receivers at the IRAM-30m telescope: 3 mm, 2 mm, 1.3 mm (lower end) and 1.3 mm (upper end). In order to have an idea in the printed version of the correspondence between data and model, we present nesting zooms in frequency in all figures, so that the most detailed panel shows 0.5 GHz wide spectra (corresponding to the frequency coverage in each observational setting). The whole survey at this level of detail needs about 300 pages of figures and tables and therefore this is available only as on-line material. Finally, Table 6 provides the position and intensity of the remaining unidentified features after the analysis performed.

3.1. *Continuum emission*

The continuum in T_A^* scale was derived from the pointing scans, as explained in section 2, after discarding a few obvious bad scans. T_{MB} and fluxes have been derived from a fit of those data to a horizontal line, scaled by the corresponding beam and forward efficiency factors of the 30m telescope (B_{eff} ranges from 0.79 to 0.42 and F_{eff} from 0.95 to 0.88 in the frequency range 80 to 275 GHz for this telescope). This analysis is not too much affected by the presence of lines because the total flux from the lines is less than 3-5 % relative to the continuum flux in most frequency settings. As a comparison, the total flux is dominated in fact by the lines in millimeter wave observations toward high mass star forming regions such as Orion (> 50% of the total flux towards the IRc2 position at these wavelengths, Tercero et al. *in prep*). A few frequency settings with very strong lines such as the lowest rotational transitions of CO and HCN have been ignored for the continuum flux analysis in CRL 618. The results were presented and discussed in sections 4.1 and 5.1, Fig1, and Table 2 of P04. In terms of T_{MB}, the continuum follows a straight line from 0.52 K at 80 GHz to 1.52 K at 275 GHz. The spectral behavior seems to be basically the same in the frequency range 280-360 GHz according to our results obtained at the Caltech Submillimeter Observatory (P04, P05).

3.2. *Overall line spectra*

The overall results of the line survey presented in figures 1, 2, 3, and 4 show that the most intense lines (above 0.2 K in T_A^*) belong to a very limited number of species (H recombination lines, C_3H_2, HCN, HCO+, CN, CO, CS, H_2CO, CH_3CN, CCH and HC_3N). They also show how, as frequency increases, the absorption part of the line profile becomes less important with respect to the emission part in species showing P-Cygni profiles, indicating that the spectral behavior of the continuum flux plays a fundamental role in the evolution of the absorption/emission ratio. The absolute energy levels of the transitions play also a role, but less important. The clustering of lines belonging to HC_3N and its isotopic and vibrationally excited species every ∼9 GHz is also nicely delineated. The detailed zoom (500 MHz) at the bottom of each figure illustrates the line identification process. Individual figures at this level of detail, including a comparison with the model, have been created for the whole data set and are available only as on-line material. Some spectra are so crowded with lines that zooms showing only 250 MHz of data have been necessary. A set of tables with the format of Table **??**, only available also as on-line material, provide the rest frequencies of all identified features and the complete quantum numbers of the transition (usually omitted in the figures due to lack of space). The labeling is quite straightforward for all molecules with the exception of HC_3N that, we should remind, is responsible for about 55% of the features seen in the survey. For this molecule the lines are labeled by the rotational quantum numbers (J_{up}–J_{low}), the vibrational quantum numbers of the four (out of seven) lowest vibrational modes (v_4,v_5,v_6,v_7) and the ℓ-doubling param-

eters for the bending modes: [ℓ_5 ℓ_6 ℓ_7]. The complete set of frequencies for this molecule has been obtained from Fayt et al. (2004), and the agreement is excellent. For HC_5N we use a similar notation with quantum numbers of the three (out of eleven) lowest vibrational modes (v_9,v_{10},v_{11}) and the necessary ℓ-doubling parameters.

3.3. *Line identification*

The line identification process has been based on J. Cernicharo's own molecular rotational line catalog. The catalog contains now ∼1300 molecules, radicals and atoms, and the number of lines in the frequency range 80-280 GHz exceeds 600000.

Although part of the line identification could be done by means of an automated procedure (mainly designed to recognize the lines from the cyanopolyynes HC_3N and HC_5N), the spectra are sometimes so crowded with lines that an important part of the identification and labeling work has to be done manually, specially taking into account that the greatest interest is usually in the weak features.

The molecular species with identified lines in the millimeter spectrum of CRL 618 are listed in Tables 4 and 5. Very few are O-bearing molecules (only SiO, H_2CO and HCO^+ in addition to CO), and there is also CS, and recombination lines of Hydrogen and Helium. The most prominent features in the spectrum are due to the cyanopolyynes family, mainly HC_3N, for which we have identified lines from more than 30 isotopic, isomeric or vibrationally excited forms. The key for deducing the basic physical parameters of CRL 618 has been to count on several hundred of lines of HC_3N with a wide range of excitation conditions to probe the different gas regions of this source (see P04 and P05).

We know nevertheless that this object has to have some relatively large carbon chains, based on the discoveries published by Cernicharo et al. (2001a,b). Compared to other cases such as Orion or IRC+10216, the number of U-lines in the CRL 618 survey is very small: Only 74 or one per ∼2.1 GHz as an average in the surveyed range. Although several species are candidates to explain a few of these U lines, their complex rotational spectrum should display other features arising above the noise level that are not seen, and therefore the assignment could not be established. Table 6 gives the frequencies and peak emission and absorption (if present) values for the unidentified features after subtracting the continuum level. The search for some particular species is described in section 3.5.

Detailed tables and figures showing the ∼3100 features that could be identified with the help of the model described in section 3.4 are available as on-line material only.

3.4. *Model*

A model aimed at reproducing the whole millimeter wave spectrum of CRL 618 as accurately as possible with the minimum number of parameters has been developed. To achieve its completion, four basic steps have been followed:

1. Model for the continuum flux considering a fixed size of the region from which it emerges, its brightness temperature at a given frequency, and a spectral index. The values used, 0.27" size, 3900 K at 200 GHz and $(\nu/\nu_0)^{-1.12}$ behavior, were found and discussed in P04.

2. Model for the inner (1.5") slowly expanding molecular envelope (*SEE*) using lines from vibrationally excited states of HC_3N (the best tool for this task). The average temperature of the region (250-275 K), HC_3N column density in front of the continuum source ($\sim 3\cdot 10^{17}$ cm^{-2}), and details about the morphology and the velocity field, were also obtained in P04.

3. Model for the high velocity wind (*HVW*), reaching ∼200 kms^{-1}, presumably quite collimated, noticeable in some abundant species such as CO, HCN and v=0 HC_3N (see P05).

4. Model for the colder and outer, with respect to the *SEE*, cold circumstellar shell (*CCS*) that is responsible for most of the rotational emission from ν_7 and v=0 HC_3N, and of v=0 HC_5N. This gas component is also dominant in the emission of several other species. The average temperature (∼30 K), position (3.0" to 4.5" diameter), velocity field, density distribution, and abundance ratio of all species with respect to HC_3N, have been obtained in P05 and PC06.

The model goes into some detail on the morphology of the object. For example, the geometry is not spherical. The *SEE* has an elongated shape, the *HVW* is collimated, and the *CCS* has a bipolar density distribution. The velocity field has both radial and azimuthal components. The azimuthal symmetry is broken because the line of sight is inclined with respect to the symmetry axis. See Fig. 4 of P04 and Fig. 3 of P05 for more details. As a result, as discussed in section 3.2 of PC06, quadratures in 4 different variables are necessary for the calculations (frequency, impact parameter, path along the line of sight, and angle in the plane perpendicular to the line of sight). All species listed in Table 4 have been included in the general calculations (except stated otherwise).

In P04, P05 and PC06, the calculations were performed for a selection of lines of each species that met several requirements such as avoiding line blendings and representing well the energy range probed by each species. This allowed us to draw a quite precise picture of the structure, physical conditions and chemical abundances in the source with reasonable computation times. Now, the model has been run for all surveyed frequencies in order to check its consistency and to be provided as a final product of this study together with the whole and labeled data set.

3.5. *Search for Trace Molecules*

As the complexity of the molecules increases, their abundances are usually lower and their partition functions larger. In order to identify a new molecule in the data, it is necessary to run a model for a large set of transitions. Our search for new species has been based on possible products from simple reactions using molecules and radicals already identified in this survey and in IR observations.

3.5.1. *C_6H radical*

The abundance of C_2H and CN in CRL 618 allows an efficient growth of $HC_{2n+1}N$ and $C_{2n}H_2$ molecules (see the detection of the polyyne chains C_2H_2, C_4H_2, and C_6H_2 in Cernicharo et al. 2001; and the polymerization of HCN in Cernicharo 2004 and P05). As a consequence, the linear radicals $C_{2n}H$, with only one free bond, are much more abundant in this object than $C_{2n+1}H$, with three free bonds. Therefore, we expected to detect the C_6H linear radical. However, the large rotational partition function of this species combined with a decrease in abundance with respect to C_4H and also the the higher energy levels of C_6H that are sounded above 80 GHz (well above the Boltzmann peak corresponding to a temperature of ∼30 K) with respect to the lighter radicals, make in fact its detectability marginal at the sensitivity level of the survey.

3.5.2. *C_5N radical*

Although the radical C_3N is more abundant than the combination of c-C_3H and l-C_3H, C_5N is not detected in the survey, contrary to C_5H. The latter is the less abundant main species detected in the survey. Assuming a similar abundance for C_5N its non detection could be explained by its lower dipole moment (3.385 Debyes instead of 4.881 Debyes for C_5H). In any case, above 80 GHz the rotational lines of both molecules are past the Boltzmann peak corresponding to the temperature of the cold circumstellar shell of CRL 618.

3.5.3. *H_2C_4 and H_2C_3 radicals*

Double C bounds seem to be rare in CRL 618 compared with carbon chains alternating single and triple bounds (as in the cyanopolyynes, polyynes and related radicals). This is further confirmed by our search of the H_2C_4 and H_2C_3 radicals (in which all carbons are doubly bounded) that has resulted on non detection for H_2C_4 and a marginal one for H_2C_3. Although some features in the spectra are located at H_2C_4 and H_2C_3 frequencies, a calculation of the whole spectrum to reproduce those features gives inconsistencies at many other frequencies (non-detections where a line should be expected).

3.5.4. *CH_2CHCN*

This is so far the only positive new finding. This molecule has μ_a=3.815 Debyes and μ_b=0.894 Debyes transitions that result on many weak features in our survey (see Fig. 2, bottom panel). We have found an abundance ∼15 times less than that of HC_3N in the *CCS*. This value is intermediate between those found for CH_3CN and CH_3CCH, although there is evidence that part of the signal detected from the last two molecules comes from the *SEE* (see PC06). The relatively similar abundances found for the three species tell us about a similar chemistry leading to their formation; see Cernicharo (2004) for details about chemical routes in CRL 618.

3.5.5. *C_6H_5CN and C_6H_5CCH*

Given the evidence in support of the detection of benzene (C_6H_6) and the large abundances of the radicals CN and CCH in CRL 618, we have checked for the presence of these two molecules but unfortunately with negative results. The large partition function of these species combined with a column density of benzene of 2×10^{15} cm^{-2} at most in this object (Cernicharo et al. 2001) in fact imply that the intensity of the lines cannot be expected to arise above the sensitivity level of the survey.

3.5.6. *CH_2CN*

This radical, that in principle could be expected to be detectable as it should be formed in similar routes to those of the abundant CH_3CN in CRL 618 has been the subject of an specific search. Only some features around 161.95 GHz and 241.35 GHz (see table 6) seem to be related to this radical, but the detection cannot be confirmed because there is no correspondence at other frequencies where a line should be expected.

3.5.7. *^{13}C substitutions of c-C_3H_2*

Starting from the abundance of c-C_3H_2 and considering a ratio $^{12}C/^{13}C$ of 40 in the *CCS*, found in P05 and PC06, it would result that $H^{13}CCCH$ at least could be detectable. Its non detection indicates that perhaps the value 40 should be understood as a lower limit. Further evidence for this is provided by $H_2^{13}CO$, ^{13}CS, ^{13}CCH, and $C^{13}CH$, that are not seen either. We should remind that the ratio $^{12}C/^{13}C$ is only about 15 in the inner *SEE*, possibly due to injection of ^{13}C-rich material generated in a late thermal pulse to the inner parts of the gas outflows of CRL 618. The result presented in this section, therefore, further strengths our (PC06) finding of quite different $^{12}C/^{13}C$ abundance ratios in the *SEE* and *CCS* regions of CRL 618.

3.6. *Comparison with PPN chemical models*

The study of Woods et al. (2003) provides chemical abundances in a region within $8.9{\cdot}10^{15}$ cm from the central star, which roughly coincides with the SEE of our model. Their predictions provide small $[HC_3N]/[HC_5N]/[HC_7N]$ ratios, just as we observed, that support the efficiency of polimerization in creating polyyne and cyanoplyyne chains in this inner SEE (already reported in P05 and in agreement with predictions in Cernicharo 2004). The predictions made in Woods et al. (2003) for radicals such as CN, CCH, C_4H, C_3N,... show relative abundances with respect to HC_3N of less than 10^{-2} (except $\sim10^{-1}$ for C_3N) which would make them very difficult to detect in the SEE. This is confirmed by our data because the emission we detect from those radicals is dominated by the CCS component (almost no signs of absorption). The reason for this is that at the densities and temperatures of the SEE, reactions with H_2 would be very efficient to transfer those radicals into polyyne or cyanopolyyne species (that dominate in this region) whereas in the much colder CCS (T∼30 K) the reactions with H_2 would barely operate.

4. CONCLUSIONS

This paper has presented the final products of the most complete spectroscopic study at millimeter wavelengths of a protoplanetary nebula carried out up to date. First, the whole data set with line identifications for about 3100 features has been presented. The number of remaining unidentified features is unprecedentedly low, only one per ∼2.1 GHz (a total of 74 in 155 GHz). Second, the whole

TABLE 1
IDENTIFIED FEATURES IN THE 80.3-115.5 GHz RANGE IN THE CRL 618 SURVEY PRESENTED IN THIS PAPER.

ν_0(MHz)	Molecule	Transition/v-state	ν_0(MHz)	Molecule	Transition/v-state
80305.928	HC_5N	J=30-29 (003)[-1]	80380.000	HC_5N	J=30-29 (003)[-3]
80388.107	l-C_3H $^2\Pi_{3/2}$	(J,F)=(7/2,4)-(5/2,3) a	80388.442	l-C_3H $^2\Pi_{3/2}$	(J,F)=(7/2,3)-(5/2,2) a
80420.646	l-C_3H $^2\Pi_{3/2}$	(J,F)=(7/2,4)-(5/2,3) b	80422.052	l-C_3H $^2\Pi_{3/2}$	(J,F)=(7/2,3)-(5/2,2) b
80446.196	HC_5N	J=30-29 (003)[1]	80559.000	U080559	
80618.000	U080618		80723.188	C_3H_2 para	$J_{K+,K-}=4_{2,2}$-$4_{1,3}$

NOTE. — Table A1 is published in its entirety in the electronic edition of the *Astrophysical Journal*. A portion is shown here for guidance regarding its form and content.

TABLE 2
IDENTIFIED FEATURES IN THE 131.2-179.1 GHz RANGE IN THE CRL 618 SURVEY PRESENTED IN THIS PAPER.

ν_0(MHz)	Molecule	Transition/v-state	ν_0(MHz)	Molecule	Transition/v-state
131256.830	MgNC	J=23/2-21/2 u	131267.422	CH_2CHCN	$J_{K+,K-}$ = $14_{0,14}$-$13_{0,13}$
131277.716	C_5H $^2\Pi_{1/2}$	J=55/2-53/2 a	131285.894	C_5H $^2\Pi_{1/2}$	J=55/2-53/2 b
131283.629	HC_5N	J=49-48 (003)[-3]	131286.219	HC_5N	J=49-48 (003)[+3]
131376.100	HC_5N	J=49-48 (003)[1]	132179.132	C_4H	J=14-13 ν_7
132246.366	$H^{13}CCCN$	J=15-14	132381.516	U132378	

NOTE. — Table A2 is published in its entirety in the electronic edition of the *Astrophysical Journal*. A portion is shown here for guidance regarding its form and content.

data set has been compared with a complete model generated from the basic physical conditions and chemical abundances deduced in the previous papers of this series (P04, P05, and PC06). Attempts have been made to search for new molecular species, not published in those works, but so far the only new finding is CH_2CHCN in the outer Cold Circumstellar Shell of CRL 618, with a chemical formation route that must be similar to those of CH_3CN and CH_3CCH. The resulting morphological, physical and chemical picture of CRL 618 that has emanated from this study is unprecendently precise thanks to the wide range of energy levels in the detected molecular lines that have subsequently been analyzed to probe the object. We have been able to provide details much beyond the angular resolution of the observations. Only interferometric observations could have provided a similar level of detail. However present-day interferometry could have concentrated on only a few lines and so a lot of information on the chemical composition would be missed. The present model can now be easily extended to the frequency range 280-360 GHz, for which another survey is almost completed with the Caltech Submillimeter Observatory. The Herschel Space Observatory will provide the opportunity to access higher frequencies into the submillimeter range with an unprecedented sensitivity and limited dilution compared with ISO. This will allow to access new molecular species and to complete the study of the continuum emission in this source. The advent of EVLA and ALMA will allow direct mapping of the structures delineated in this work and the possibility of a nearly continuous coverage from 300 MHz to 950 GHz. The large collecting area should allow to extend our view of the chemical system.

We acknowledge the support of the IRAM-30m staff during the long completion of the line survey. This work has also been supported by Spanish DGES and PNIE grants ESP2002-01627, AYA2002-10113-E and AYA2003-02785-E.

APPENDIX

ONLINE MATERIALS

Tables A1, A2 and A3 contain the identified features in the CRL 618 millimeter wave survey in the following frequency ranges: 80.3-115.5 GHz, 131.2-179.1 GHz, and the 204.5-276.0 GHz. Also included are online only figures showing the millimeter spectra.

REFERENCES

Asplund, M., Lambert, D. L., Kipper, T., Pollacco, D., Shetrone, M. D., 1999, A&A, 343, 507.
Bujarrabal, V., Alcolea, J., Sánchez-Contreras, C., Sahai, R., 2002, A&A, 389, 271
Cernicharo, J., Guélin, M., Martín-Pintado, J., Peñalver, J., Mauersberger, M., 1989, A&A, 222, L1
Cernicharo, J., Barlow, M. J., Gonzalez-Alfonso, E., Cox, P., et al., 1996, A&A, 315, L201.
Cernicharo, J., Guélin, M., Kahane, C., 2000, A&A Suppl., 142, 181.
Cernicharo, J., Heras, A. M., Tielens, A.G.G.M., Pardo, J. R., Herpin, F., Guélin, M., Waters, L.B.F.M. 2001, Ap.J. 546, L123.
De Marco, O., Bond, H.E., Harmer, D., Fleming, A.J., 2004, ApJ, 602, L93
Fayt, A., Vigouroux, C., Willaert, F. Margules, L. Constantin, L.F., Demaison, J., Pawelke, G. Mkadmi, E.B., Buerger, H., 2004, J. Mol. Spectrosc. 295, 695
Frank, A., Blackman, E.G., 2004, ApJ, 614, 737
Huggins, P.J., Manley, S.P., 2005, PASP, 117, 665

TABLE 3
IDENTIFIED FEATURES IN THE 204.5-276.0 GHz RANGE IN THE CRL 618 SURVEY PRESENTED IN THIS PAPER.

ν_0(MHz)	Molecule	Transition/v-state	ν_0(MHz)	Molecule	Transition/v-state
204788.938	c-C_3H_2	$J_{K+,K-} = 2_{2,0}$-$3_{1,0}$	204970.268	HC_5N	J=77-76
205003.000	U205003		205018.109	CH_3CCH	J=12-11 K=4
205045.497	CH_3CCH	J=12-11 K=3	205065.067	CH_3CCH	J=12-11 K=2
205076.813	CH_3CCH	J=12-11 K=1	205307.362	HC_5N	J=77-76 (001)[-1]
205308.360	HC_5N	J=77-76 (010)[-1]	205385.073	HC_5N	J=77-76 (010)[+1]

NOTE. — Table A3 is published in its entirety in the electronic edition of the *Astrophysical Journal*. A portion is shown here for guidance regarding its form and content.

Cernicharo, J, Heras, A. M., Pardo, J. R., Tielens, A.G.G.M., Guélin, M., Dartois, E., Neri, R., Waters, L.B.F.M., 2001, Ap.J. 546, L127.
Cernicharo, J., 2004, Ap.J., 608, L41.
avis, C.J., Smith, M.D., Gledhill, T.M., Varricatt, W.P., 2005, MNRAS, 360, 104.
Herpin, F., Goicoechea, J.R., Pardo, J.R., Cernicharo, J. 2002, Ap.J., 577, 961
Pardo, J.R., Cernicharo, J., Goicoechea, J.R., Phillips, T.G., 2004, Ap.J., 615, 495.
Pardo, J.R., Cernicharo, J., Goicoechea, J.R., 2005, Ap.J., 628, 275
Pardo, J.R., Cernicharo, J., 2006, Ap.J., in press.
Pavlenko, Ya. V., Geballe, T. R., Evans, A., Smalley, B., Eyres, S. P. S., Tyne, V. H., Yakovina, L. A., 2004, A&A, 417, L39.
Remijan, A.J., Wyrowski, F., Friedel, D.N., Meier, D.S., Snyder, L.E., 2005, Ap.J., 626, 233.
Sánchez-Contreras, C., Sahai, R., Gil de Paz, A., 2002, Ap.J., 578, 269
Sánchez-Contreras, C., and Sahai, R., 2004, Ap.J., 602, 960.
Woods, P.M., Millar, T.J., Herbst, E., and Zijlstra, A.A., 2002 A&A, 402, 189.

TABLE 4
CYANOPOLYYNE SPECIES INCLUDED IN THE MODEL AND J_{up} AND/OR E_{up} RANGE IN WHICH THEY APPEAR IN THE DATA. WE SEPARATE ISOTOPIC SUBSTITUTIONS AND VIBRATIONALLY EXCITED STATES (THEIR VIBRATIONAL ENERGY IS ALSO GIVEN) OF THOSE SPECIES FOR WHICH SEVERAL OF THEM HAVE BEEN DETECTED.

Molecule and vib. state	E_{vib} (cm^{-1})	J_{up} range	Range E_{rot} (cm^{-1})	Total Num. of labels	[X]/[HC_3N] in *SEE*	[X]/[HC_3N] in *HVW*	[X]/[HC_3N] in *CCS*
HC_3N (0000)		9-30	15-205	17	0.4092	0.2325	0.9905
HC_3N (0001)	223	9-30	15-205	34	0.2412	0.1859	0.0095
HC_3N (0002)	446	9-30	15-205	51	0.1065	0.1115	-
HC_3N (0010)	499	9-30	15-205	34	0.0531	0.0598	-
HC_3N (0100)	663	9-30	15-205	34	0.0216	0.0304	-
HC_3N (0003)	669	9-30	15-205	68	0.0418	0.0594	-
HC_3N (0011)	721	9-30	15-205	68	0.0313	-	-
HC_3N (1000)	880	9-30	15-205	17	0.0033	-	-
HC_3N (0101)	886	9-30	15-205	68	0.0127	-	-
HC_3N (0004)	892	9-30	15-205	77	0.0154	-	-
HC_3N (0012)	944	9-30	15-205	100	0.0138	-	-
HC_3N (0020)	998	9-30	15-205	49	0.0052	-	-
HC_3N (1001)	1103	11-30	24-205	27	0.0019	-	-
HC_3N (0102)	1109	11-30	24-205	88	0.0056	-	-
HC_3N (0005)	1115	11-30	24-205	66	0.0054	-	-
HC_3N (0110)	1162	11-30	24-205	62	0.0029	-	-
HC_3N (0013)	1168	12-30	29-205	98	0.0055	-	-
HC_3N (0021)	1221	15-30	46-205	64	0.0031	-	-
HC_3N (1002)	1326	15-30	46-205	26	0.0009	-	-
HC_3N (0103)	1332	15-30	46-205	90	0.0023	-	-
HC_3N (0006)	1338	15-30	46-205	22	0.0019	-	-
HC_3N (1010)	1379	16-30	53-205	9	0.0004	-	-
HC_3N (0111)	1385	17-30	60-205	57	0.0017	-	-
HC_3N (0014)	1431	17-30	60-205	56	0.0016	-	-
HC_3N (0022)	1464	19-30	75-205	55	0.0012	-	-
HC_3N (0030)	1497	23-30	111-205	20	0.0005	-	-
HC_3N (1100)	1543	23-27	111-165	5	0.0002	-	-
HC_3N (0201)	1549	23-30	111-205	19	0.0005	-	-
HC_3N (1003)	1549	23-29	111-191	14	0.0003	-	-
HC_3N (0104)	1555	23-29	111-191	21	0.0008	-	-
HC_3N (1011)	1602	24-30	121-205	8	0.0003	-	-
HC_3N (0112)	1608	26-30	142-205	21	0.0007	-	-
HC_3N (0015)	1608	26	142-154	1	0.0007	-	-
$H^{13}CCCN$ (0000)		10-31	20-218	18	0.0273	0.0155	0.0248
$HC^{13}CCN$ (0000)		9-30	15-205	17	0.0273	0.0155	0.0248
$HCC^{13}CN$ (0000)		9-30	15-205	17	0.0273	0.0155	0.0248
$H^{13}CCCN$ (0001)	223	10-31	20-218	36	0.0161	-	-
$HC^{13}CCN$ (0001)	223	9-30	15-205	34	0.0161	-	-
$HCC^{13}CN$ (0001)	223	9-30	15-205	35	0.0161	-	-
$H^{13}CCCN$ (0002)	446	16-30	53-205	8	0.0071	-	-
$HC^{13}CCN$ (0002)	446	17-26	60-154	9	0.0071	-	-
$HCC^{13}CN$ (0002)	446	16-28	53-178	13	0.0071	-	-
$H^{13}CCCN$ (0010)	499	12-30	29-205	26	0.0035	-	-
$HC^{13}CCN$ (0010)	499	10-30	20-205	32	0.0035	-	-
$HCC^{13}CN$ (0010)	499	10-30	20-205	29	0.0035	-	-
$H^{13}CCCN$ (0003)	669			1	0.0028	-	-
HCCNC		10-29		15	20-191	-	0.0250
TOTAL HC_3N				1736			
HC_5N v=0		31-104	39-485	55	0.0132	-	0.2794
HC_5N ν_{11}	105	31-104	39-485	118	0.0149	-	0.0451
HC_5N $2\nu_{11}$	210	31-104	39-485	147	0.0126	-	0.0055
HC_5N ν_{10}	230	31-104	39-485	105	0.0075	-	0.0023
HC_5N $3\nu_{11}$	315	31-95	39-402	152	0.0094	-	0.0006
HC_7N v=0		72-102	102-198	26	-	-	0.0503
HC_7N ν_{15}	62	79	113-116	1	-	-	0.0052
TOTAL $HC_{2n+1}N$				2340			

TABLE 5
Other molecules included in the model, presented as in Table 4.

Molecule and vib. state	E_{vib} (cm^{-1})	J_{up} range	Range E_{rot} (cm^{-1})	Total Num. of labels	[X]/[HC_3N] in *SEE*	[X]/[HC_3N] in *HVW*	[X]/[HC_3N] in *CCS*
CO		1-2	0-12	2	-	667	100
^{13}CO		1-2	0-11	2	2.5	-	2.5
$C^{17}O$		1-2	0-11	2	0.3	-	0.3
$C^{18}O$		1-2	0-11	2	0.2	-	0.2
HCO^+		1-3	0-18	3	0.1	0.2	0.1
$H^{13}CO^+$		1-3	0-18	3	-	-	0.003
HOC^+				1			
HCN		1-3	0-18	3	2.0	2.0	1.5
HCN $\nu 2$	712	1-3	0-18	5			
$H^{13}CN$		1-3	3-17	3	0.133	0.133	0.033
$H^{13}CN$ $\nu 2$		1-3		5			
HNC		1-3	0-18	2	0.2	0.2	0.167
HNC $\nu 2$	477	1-3	3-18	2			
$HN^{13}C$		1-3	0-18	3	0.013	0.01	0.004
H_2CO		-	0.64	9	-	-	0.125
SiO		2-6	1-30	4	-	-	0.013
CS		2-5	2-35	3	-	-	0.125
N_2H^+		1-1	0-3	1	-	-	0.025
c-C_3H_2			2-134	67	-	-	0.36
MgNC		7-14	8-36	16	-	-	0.10
CH_3CN		5-15	9-300	56	0.067	0.100	0.033
CH_3CCH		5-16	6-315	65	1.0	2.0	0.200
CH_2CHCN				120			0.067
CN		1-2	0-11	26	-	-	4.0
^{13}CN		1-2	0-11	24	-	-	0.25
CCH		1-3	0-18	17	-	-	0.5
C_3N		9-22	14-77	26	-	-	0.118
c-C_3H			0-41	25	-	-	0.050
l-C_3H			5-52	58	-	-	0.017
C_4H		9-29	14-142	30	-	-	1.0
C_4H ν_7	134	9-22	12-86	31	-	-	
C_5H		-	23-100	38	-	-	0.005
H_2C_3	-	-	-	2	-	-	<0.005
TOTAL no-$HC_{2n+1}N$				666			
H recombination				44			
He recombination				3			
U-lines				74			
TOTAL LABELS				**3127**			

TABLE 6
UNIDENTIFIED FEATURES IN THE 80-276 GHz IRAM-30M SURVEY OF CRL 618. FREQUENCY GIVEN IN MHz. AREA (A) GIVEN IN K·KMS^{-1} AND HPLW (W) GIVEN IN KMS^{-1}. THE σ OF THE FEATURE HAS BEEN ESTABLISHED FROM THE FOLLOWING AVERAGE RMS OF THE DATA: 4 MK AT 3 MM, 8 MK AT 2 MM, 11 MK FROM 204 TO 240 GHz, AND 14 MK ABOVE 240 GHz. ONLY 74 UNIDENTIFIED FEATURES ARISE ABOVE THE 3σ LIMIT.

Freq. MHz	A (W) σ K km s^{-1} (km s^{-1})	Freq. MHz	A (W) σ K km s^{-1} (km s^{-1})
80559	0.129 (18) 3σ	80618	0.069 (7) 3σ
83659	0.380 (24) 4σ	85136	0.295 (16) 5σ
87013	0.160 (17) 3σ	89120	0.124 (9) 4σ
89600[1]	0.239 (27) 3σ	89820	0.124 (9) 4σ
91156	-0.320 (20) 4σ	91238[2]	-0.082 (5) 4σ
91383	0.389 (21) 5σ	91441[2]	0.100 (9) 3σ
92414[2]	-0.105 (4) 7σ	92814[3]	-0.147 (7) 5σ
95667	0.289 (23) 3σ	97637	0.447 (48) 3σ
97728	0.167 (17) 3σ	97772	0.246 (22) 3σ
98822	0.301 (27) 3σ	98856	0.392 (34) 3σ
100265	0.304 (18) 4σ	100540	0.530 (37) 4σ
101372	-0.115 (5) 6σ	101751	0.212 (14) 4σ
102222	0.261 (18) 4σ	103426	0.160 (17) 3σ
103910[4]	0.237 (19) 3σ	107121[5]	0.281 (24) 3σ
107275	0.310 (25) 3σ	107620	0.377 (31) 3σ
115426	0.675 (19) 9σ	132378	0.22/-0.49 (9/27) 4σ
132679	0.735 (52) 3σ	134239	0.248 (11) 3σ
134525	0.488 (28) 3σ	137291	-0.121 (4) 4σ
137720	0.446 (15) 4σ	141811	0.117 (8) 3σ
142293	0.165 (9) 3σ	146210	0.445 (17) 3σ
150349	-0.054/-0.055 (3/6) 3σ	150620	0.470 (42) 3σ
160670	0.835 (27) 4σ	160952[6]	3.669 (56) 9σ
170642	0.847 (35) 3σ	172998	-0.092 (4) 3σ
173106	-0.389 (15) 3σ	173572	-0.130 (6) 3σ
175840	0.057 (2) 3σ	205003[7]	-
218042	1.144 (17) 6σ	218207	1.640 (17) 9σ
219270	0.575 (18) 3σ	220431	0.556 (17) 3σ
221366	2.132 (59) 3σ	221980[7]	3.612 (28) 11σ
228507	0.105 (3) 3σ	234936	0.693 (11) 5σ
235597	0.422 (16) 3σ	235606	0.152 (6) 3σ
241337[8]	3.799 (45) 7σ	241388[8]	1.175 (19) 5σ
241498	0.913 (15) 5σ	242642	0.178 (5) 3σ
245120	0.690 (17) 3σ	248647	0.139 (4) 3σ
249111	0.487 (17) 3σ	256428	0.238 (4) 5σ
258314	0.811 (15) 4σ	260295	0.293 (6) 4σ
260426	0.233 (5) 3σ	263475	0.328 (8) 3σ
263840	0.186 (4) 3σ	272988	1.560 (11) 10σ

[1] (id) $HC^{13}CCCCN$ J=34-33
[2] (cm) only one channel
[3] (id) C_3H_2
[4] (id) H 56γ
[5] (id) HC_5N $3\nu_{10}(1+)$ J=40-39
[6] (id) CH_2CN J=8-7
[7] (bl) CH_3CCH
[8] (id) CH_2CN J=12-11
id: possible identification; cm: comment; bl: existing blending

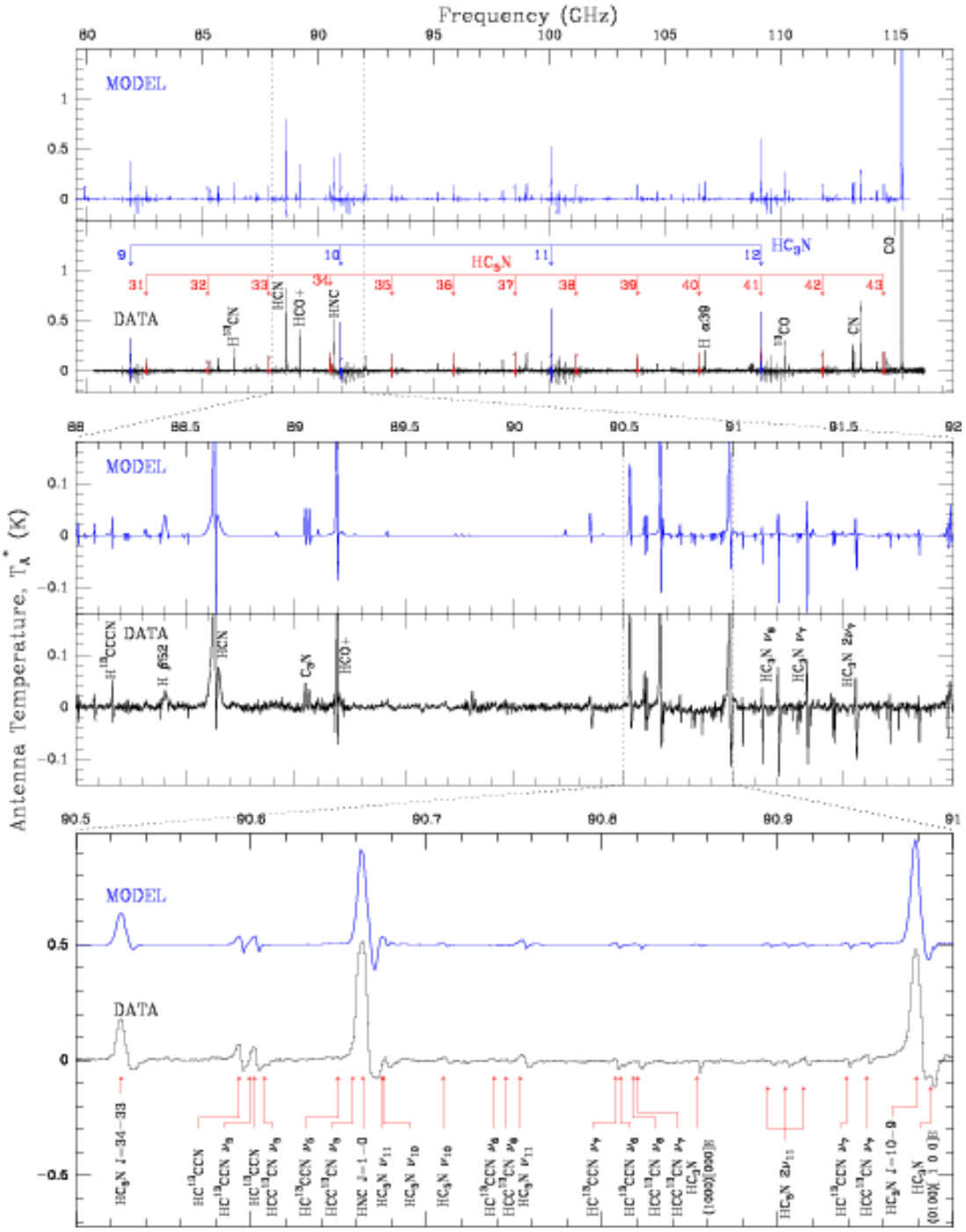

FIG. 1.— Results of the CRL 618 IRAM-30m survey in the frequency range 80.0-116.5 GHz (3 mm window) compared to the model devepoloped according to the results found in the series of papers P04, P05 and PC06. We include nesting zooms on intervals covering 4 GHz and 0.5 GHz respectively. The data are shown in terms of T_A^* with the continuum level substracted. The labels next to the arrows in the upper panel indicate the J_{up} number of the corresponding HC_3N or HC_5N transition. The complete set of detaliled figures at 0.5 GHz intervals with line identifications (similar to the lower panel), is available as on-line material only.

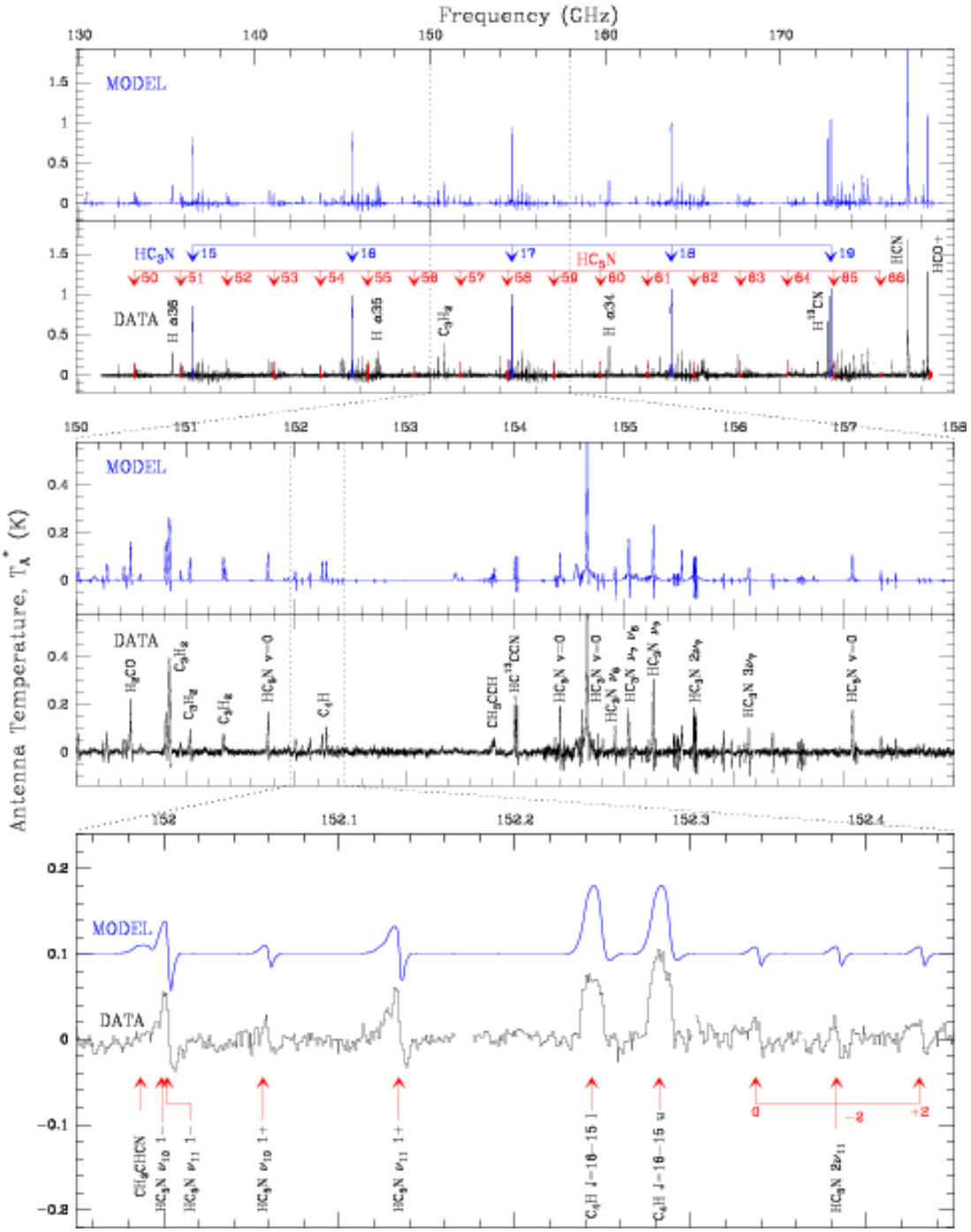

FIG. 2.— Same as previous figure but for the frequency range 130.5-179.0 GHz (2 mm window). The first zoom shows 8 GHz instead of 4.

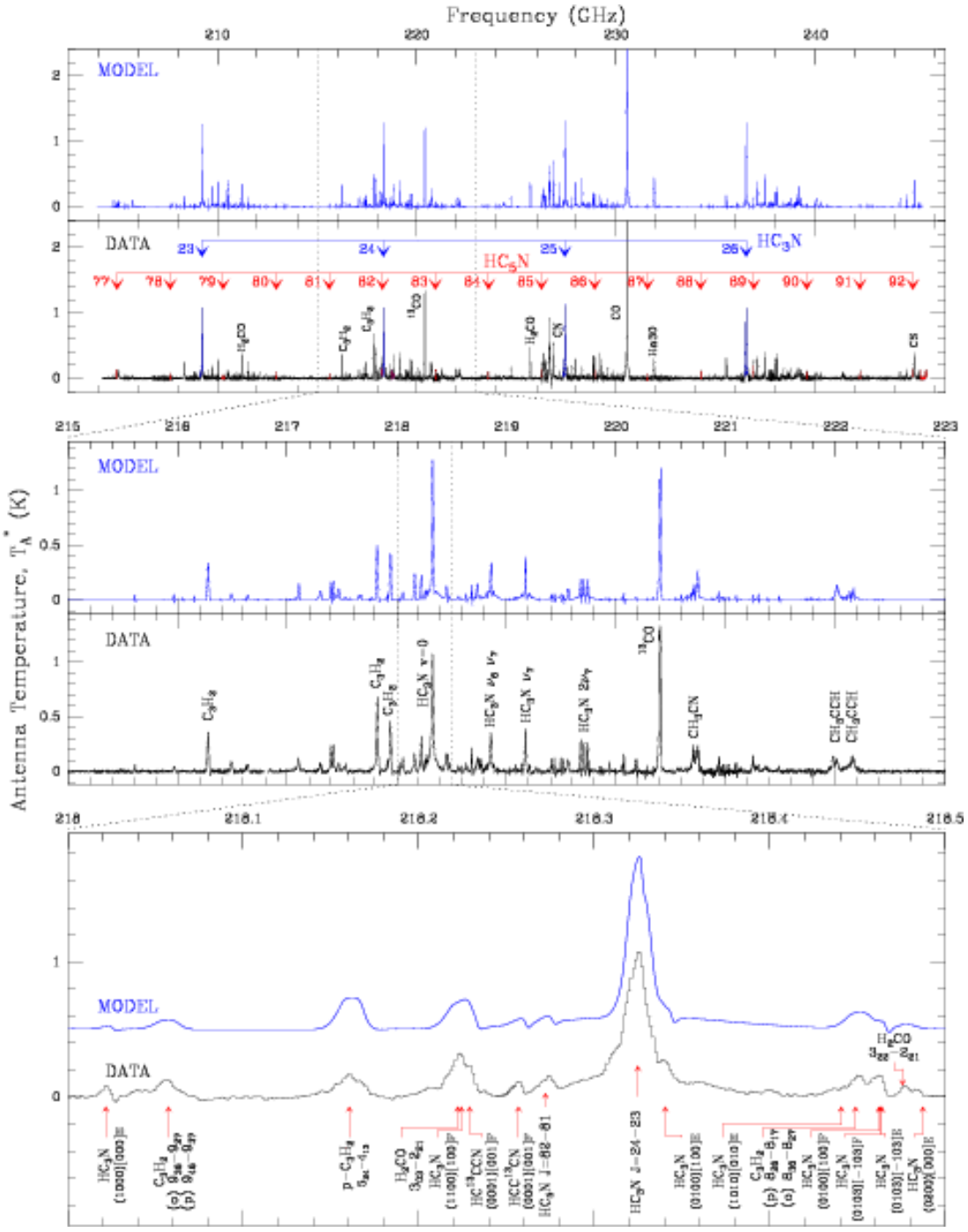

FIG. 3.— Same as previous figure but for the frequency range 204.5-245.0 GHz (lower part of the 1.3 mm window).

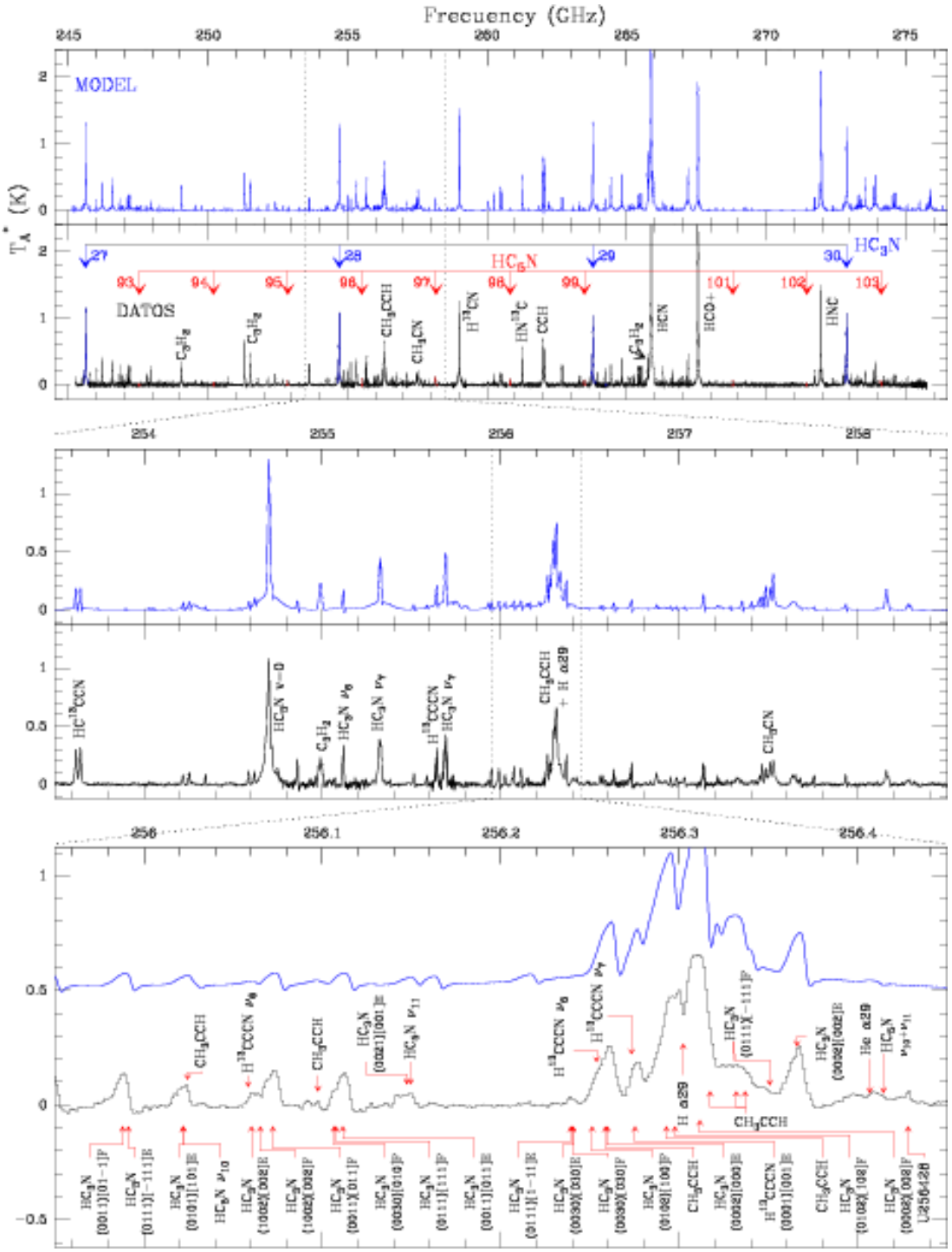

FIG. 4.— Same as previous figure but for the frequency range 245.0-275.5 GHz (upper part of the 1.3 mm window).